Sci. 1967, 37, 743] and Fourier program FFSYNT [J. Appl. Crystallogr. 1973, 6, 246]. Johnson's ORTEP thermal ellipsoid plotting program was used for drawing.
(18) Muetterties, E. L.; Guggenberger, L. J. J. Am. Chem. Soc. 1974, 96, 1748.
(19) Raymond, K. N.; Corfield, P. W. R.; Ibers, J. A. Inorg. Chem. 1968, 7, 1362.
(20) Allen, G. C.; Hush, N. S. Inorg. Chem. 1967, 6, 4.
(21) Ray, N.; Hulett, L.; Sheanan, R.; Hathaway, B. Inorg. Nucl. Chem. Lett. 1978, 14, 305.
(22) Figgis, B. N.; Lewis, J. Adv. Inorg. Chem. 1964, 6.
(23) Boudreaux, E. A. Trans. Faraday Soc. 1963, 59, 1055.
(24) Ferraro, J. R. "Low-Frequency Vibrations of Inorganic and Coordination Compounds"; Plenum Press: New York, 1971.
(25) Nakamoto, K. "Infrared and Raman Spectra of Inorganic and Coordination Compounds"; Wiley: New York, 1978.
(26) Bellamy, L. J. "The Infra-Red Spectra of Complex Molecules"; Chapman and Hall: London, 1975; pp 267–291.
(27) Colthrum, N. B.; Daly, L. H.; Wiberley, S. E. "Introduction to Infrared and Raman Spectroscopy"; Academic Press: New York, 1975; p 282.
(28) Vallarino, L. M.; Goedken, V. L.; Quagliano, J. V. Inorg. Chem. 1973, 12, 102.

Lifetimes, Spectra, and Quenching of the Excited States of Polypyridine Complexes of Iron(II), Ruthenium(II), and Osmium(II)

Carol Creutz,* Mei Chou, Thomas L. Netzel, Mitchio Okumura,[1] and Norman Sutin*

Contribution from the Chemistry Department, Brookhaven National Laboratory, Upton, New York 11973. *Received April 23, 1979*

Abstract: The lifetimes of the excited states formed by 530-nm excitation of polypyridine complexes of iron(II) (FeL_3^{2+}) and osmium(II) (OsL_3^{2+}) have been determined by laser flash-photolysis techniques. The FeL_3^{2+} lifetimes, measured in water at room temperature using picosecond absorption spectrometry, are as follows (L, $\tau \pm \sigma$ (ns)): 2,2′,2″-terpyridine (2.54 ± 0.13); 2,2′-bipyridine (0.81 ± 0.07); 4,4′-dimethyl(2,2′-bipyridine) (0.76 ± 0.04); 1,10-phenanthroline (0.80 ± 0.07); 4,7-(diphenyl sulfonate)-1,10-phenanthroline (0.43 ± 0.03). Lifetimes for the analogous complexes of osmium(II) lie in the range 10–100 ns under the same conditions. Unlike the excited states of $Ru(bpy)_3^{2+}$ and $Os(bpy)_3^{2+}$ (λ_{max} 430–460 nm, $\epsilon \sim 5 \times 10^3$ M^{-1} cm^{-1}), the excited state of $Fe(bpy)_3^{2+}$ does not luminesce or absorb significantly in the visible ($\epsilon < 10^3$ M^{-1} cm^{-1} at $\lambda \geq 350$ nm) but does exhibit intense absorption below ~325 nm. Rate constants for the quenching of the excited states of polypyridine complexes of osmium(II) and ruthenium(II) by ground-state polypyridine complexes of iron(II), ruthenium(II), and osmium(II) are reported and are ascribed to either electron-transfer or energy-transfer processes. The excited states of tris(2,2′-bipyridine)iron(II) and of bis(2,2′,2″-terpyridine)iron(II) undergo reaction with Fe_{aq}^{3+} (0.5 M H_2SO_4, 25 °C) with a rate constant $\leq 1 \times 10^7$ M^{-1} s^{-1}. Based on a comparison of its properties with those of the luminescent charge-transfer excited states of ruthenium(II) and osmium(II) polypyridine complexes the excited state of FeL_3^{2+} is identified as a ligand-field state. The potential of the excited-state couple $Fe(bpy)_3^{3+} + e = {}^*Fe(bpy)_3^{2+}$ is estimated to be +0.1 V.

Introduction

The photophysics and photochemistry of polypyridine complexes of ruthenium, especially tris(2,2′-bipyridine)-ruthenium(II) ($Ru(bpy)_3^{2+}$), have been extensively investigated in recent years.[2] Both kinds of study have implicated a major role for the luminescent metal-to-ligand charge-transfer excited state of complexes of this family. Similar conclusions have been drawn for the luminescent osmium(II) polypyridine complexes, although fewer data are available for this series.[3-7] By contrast, the analogous complexes of iron(II) have received relatively little attention. Fink and Ohnesorge[8] have found that FeL_3^{2+} complexes (L = bpy, 1,10-phenanthroline = phen, 2,2′,2″-terpyridine = terpy, 2-methyl-1,10-phenanthroline) do not luminesce in absolute ethanol at either room temperature or 80 K. Kirk et al.,[9] using picosecond absorption spectrometry, determined a 0.83-ns lifetime for a nonemitting excited state of $Fe(bpy)_3^{2+}$, while Street et al.[10] have made analogous measurements on $Fe(phen)_3^{2+}$. Chum et al.[11] have obtained evidence for photoinduced oxidation of iron(II) chelates, including $Fe(bpy)_3^{2+}$, in aluminum chloride–ethylpyridinium bromide melts, while Phillips et al.[12] have reported that $Fe(bpy)_3^{2+}$ undergoes photooxidation in the presence of Fe_{aq}^{3+}.

In this work we have used laser flash-photolysis techniques to measure the lifetimes and spectra of the excited states of polypyridine complexes of ruthenium(II), osmium(II), and iron(II). In addition we have studied the quenching of the excited states of the osmium(II) and ruthenium(II) complexes by ground-state polypyridine complexes of iron(II), ruthenium(II), and osmium(II) and the quenching of $Fe(bpy)_3^{2+}$ and $Fe(terpy)_2^{2+}$ by Fe_{aq}^{3+} ions. The mechanisms of these reactions and the properties of the excited states of the iron(II) complexes are discussed below.

Experimental Section

Materials. The polypyridine ligands were used as received from the G. F. Smith Co. or from Fisher. The method of preparation of the osmium polypyridine complexes followed that given by Dwyer and co-workers.[13] The procedure for $Os(bpy)_3I_2$ is typical: 1.0 g of K_2OsCl_6 and 1.28 g of 2,2′-bipyridine were mixed with 50 mL of glycerol and heated at 240 °C for 1 h. The hot glycerol mixture was poured into 150 mL of hot water and then acidified with ~10 mL of 5 M HCl. The green solution was filtered, and solid potassium iodide was added to the filtrate. The resulting black powder was separated by filtration and washed with cold water and ether. The perchlorate salt was prepared from the iodide as follows. A 10% solution of sodium perchlorate was added dropwise to a solution of the iodide salt in hot water. The wall of the container was scratched with a glass rod and the solution was cooled in an ice bath. The solid perchlorate was collected on a filter, washed with ether, then dried in vacuo overnight. The purity of the products was ascertained by analysis for Os and halogen. When it proved difficult to separate OsL_3^{2+} from unreacted ligand L (L, a phenanthroline derivative), the impure OsL_3X_2 was digested with benzene in order to dissolve the excess ligand.

Stock (0.01 M) solutions of the iron(II) polypyridine complexes were prepared by mixing 1.0 mmol of $Fe(NH_4)_2(SO_4)_2$, 3.1 mmol of

0002-7863/80/1502-1309$01.00/0 © 1980 American Chemical Society

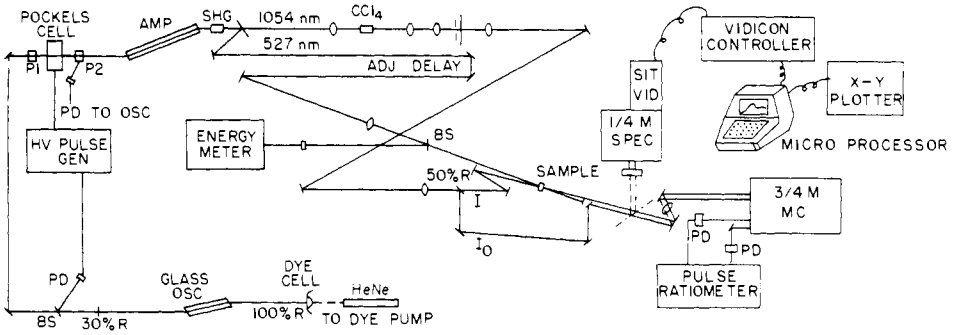

Figure 1. Picosecond absorption spectrometer: R, reflector; GLASS OSC, Nd/glass laser oscillator; BS, beam splitter; PD, photodiode; P1 and P2, crossed polarizers; PD TO OSC, fast photodiode signal to a 519 oscilloscope; AMP, Nd/glass amplifier; SHG, second harmonic generating crystal; CCl_4, 5-cm path length cell of carbon tetrachloride; ADJ DELAY, translation stage with 1 m of travel; I and I_0, paths of the white light pulses through the sample and reference cells, respectively; SIT VID, silicon intensified-target vidicon; ¼ m SPEC, ¼ m spectrograph; ¾ m MC, ¾ m monochromator. The dashed lines indicate the beam paths when the vidicon detection system is used. A 1-mm aperture and ground-glass diffuser plate are used after the CCl_4 cell to homogenize the white light pulses.

ligand (for FeL_3^{2+} complexes), and a spatula tipful of ascorbic acid and diluting to 100 mL. The solutions were characterized spectrally[14] and stored in the dark under argon, then diluted to the desired concentration with water before use.

Lifetimes of the OsL_3^{2+} Compounds. Solutions 10^{-5}-10^{-4} M in OsL_3^{2+} (ϵ_{530} typically 5×10^3 M^{-1} cm^{-1}) were excited using a 5- or 8-ns (full width at half-height) pulse of 530-nm light from a frequency-doubled neodymium laser. The basic laser, frequency doubling, and detection systems have been described previously.[15,16] (The Q-switched 22-ns pulse was, however, sliced to give a shorter pulse: the diameter of the oscillator pulse was reduced to 0.5 cm by the installation of a glass diaphragm within the oscillator cavity and a Korad Model KQS4 optical gate was inserted between the oscillator and the amplifier head. The spark gap which opened the gate was routinely operated at 20 kV and 60 psi of nitrogen. Approximately 100 mJ 530-nm pulses (after doubling) could be obtained under optimal conditions. Emission associated with the decay of the OsL_3^{2+} excited states was monitored at ~715 nm using a Hamamatsu R928 photomultiplier.

Measurement of the $Ru(bpy)_3^{2+}$, $Os(bpy)_3^{2+}$, and $Fe(bpy)_3^{2+}$ Excited-State Spectra. Deaerated solutions of $Ru(bpy)_3^{2+}$, $Os(bpy)_3^{2+}$, or $Fe(bpy)_3^{2+}$ contained in a 1 × 1 cm "microcell" (interrogation path length 0.37 cm)[16] were excited with a pulse of 530-nm light.[15,16] For $Os(bpy)_3^{2+}$ the absorbance changes observed immediately following the 8-ns excitation pulse were recorded as a function of wavelength at high excitation intensity (≥20 einsteins cm^{-2} s^{-1}, see below) at 10- or 15-nm intervals. For $Ru(bpy)_3^{2+}$ the absorbance changes following a 22-ns excitation pulse were similarly determined. The spectrum of $*Fe(bpy)_3^{2+}$ was measured in an analogous fashion using the same apparatus as above, but in this work the absorbance changes taking place during a 22-ns excitation pulse were measured. In calculating the absolute spectrum of $*M(bpy)_3^{2+}$, the directly determined absorbance changes (ΔA, defined as postflash absorbance—or, in the case of $*Fe(bpy)_3^{2+}$, maximum absorbance attained during flash—minus preflash absorbance A_0) were corrected for the ground-state bleaching (c^*A_0/c_0, where c^* is the excited-state concentration and c_0 is the preflash ground-state concentration) to give the excited-state absorbance A^* according to the equation

$$A^* = \Delta A + \frac{c^*}{c_0} A_0 \qquad (1)$$

The value of A_0 was determined using the flash-photolysis monitoring optics (i.e., same wavelength, slit width, sample cell, etc., as for ΔA). The evaluation of c^*/c_0 is described in the Results section. Typical excitation intensities in this experiment were 2 to 5×10^1 einsteins cm^{-2} s^{-1}.

Measurement of 530-nm Excitation Intensities. The relative laser pulse intensity was monitored routinely by diverting a small fraction of the 530-nm beam into a photodiode (EG&G) whose output was displayed on a storage oscilloscope or monitored with a Laser Precision Corp. Energy Ratiometer (Rk 3232) with digital display. Two approaches were used in estimating the absolute excitation intensities. In the first, the pulse was collected in a Control Data thermopile (TRG 117) and the thermopile output was measured with a Keithley 150 B Microvoltmeter (41 μV J^{-1}, 4.4×10^{-6} einstein J^{-1} at 530 nm). The area of the focused laser beam was determined by burning a photograph positioned at the front of the photolysis sample cell. In the second method eq 2 was applied:

$$c^*/c_0 = 1 - \exp(-2.3 \times 10^3 \epsilon \phi^* I_0 \Delta t) \qquad (2)$$

(See Appendix for the derivation of eq 2.) Here c^* is the concentration of excited state after the laser pulse, c_0 is the ground-state concentration before the pulse, ϵ is the molar absorptivity of the ground state at the excitation wavelength, ϕ^* is the quantum yield for production of the excited state, and the product $I_0\Delta t$ is the number of moles of photons per square centimeter per pulse. The quantity c^*/c_0 was evaluated for a solution 1.0×10^{-4} M in $Ru(bpy)_3^{2+}$ and 5.2×10^{-3} M in Fe_{aq}^{3+} in 1 N H_2SO_4[3,15] as a function of laser intensity by monitoring the magnitude of the absorbance decrease at 490 nm.[16] These data were plotted as $\ln(1 - c^*/c_0)$ vs. relative excitation intensity to give linear plots; the slopes of these plots provided an absolute calibration of the monitoring photodiode. The laser pulse shape and duration were determined by deflecting part of the doubled light into a photodiode (Korad Laser systems Model KD1) whose output was displayed on a Tektronix 7834 storage oscilloscope.

Quenching Rate Constants. Rate constants (k_q) for quenching of $*RuL_3^{2+}$ and $*OsL_3^{2+}$ were determined for solutions 2 to 5×10^{-5} M in RuL_3^{2+} or OsL_3^{2+} and 0 to 5×10^{-3} M in quencher. The lifetimes of $*ML_3^{2+}$ in the absence (τ_0) and presence (τ) of quencher were determined as a function of quencher concentration [Q]. Rate constants were evaluated from the slopes of plots of $(\tau_0/\tau) - 1$ vs. [Q]; slope = $k_q\tau_0$. The range of media used was dictated by the solubilities of the polypyridine complexes.

Lifetimes of the FeL_3^{2+} Complexes. Lifetimes for ground-state repopulation of the iron(II) polypyridine complexes were measured using picosecond absorption spectroscopy.[17,18] Figure 1 shows a schematic diagram of the experimental apparatus. A Nd-glass laser (1-ppm repetition rate) was mode locked by flowing a dichloroethane solution of Kodak 9860 dye through a cell in optical contact with the rear mirror of the cavity. A single pulse was selected with a Pockels cell energized by a Lasermetrics high-voltage pulse generator. The rejected pulses were directed to a high-speed photodiode coupled to a Tektronix 519 oscilloscope. Every laser shot was monitored and data were accepted only if the laser output consisted of a single train. The selected pulse of 1054-nm light was amplified to about 60 mJ of energy. Approximately 10% of this energy was converted to the second harmonic in a KDP (potassium hydrogen phosphate) crystal. The remaining 1054-nm light was focused into a 5-cm cell of either D_2O or carbon tetrachloride to produce white light.[19,20] The white light extended from about 420 nm to beyond 850 nm and its energy was about 0.1 nJ/nm from 500 to 600 nm. To image the continuum light in the photolysis region of the sample, it was focused onto a ground glass diffuser plate located behind a 1-mm diameter aperture. The diffuser smoothed out spatial inhomogeneities in the continuum beam. A lens positioned at twice its focal length from both the sample and the monochromator relayed the continuum to the entrance slit of the spectrograph and onto the detector. Recently a 0.25-m double monochromator with subtractive dispersion has been inserted between the sample and the dispersing spectrograph and has significantly reduced the magnitude of scattered excitation light. The 400-500-nm measurements on $Fe(phen)_3^{2+}$ were made after these improvements.

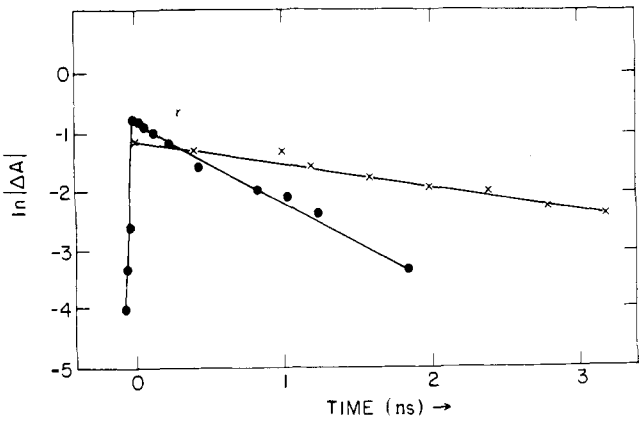

Figure 2. Kinetic data for the restoration of ground-state absorbance at 557 nm for $Fe(terpy)_2^{2+}$ (crosses) and $Fe(4,4'\text{-}(CH_3)_2bpy)_3^{2+}$ (solid circles). The natural logarithm of the absolute value of $A_\infty - A_t$ (absorbances at times infinity and t, respectively) is plotted vs. time. For $Fe(bpy)_3^{2+}$ the points at "negative" time indicate the excitation pulse width.

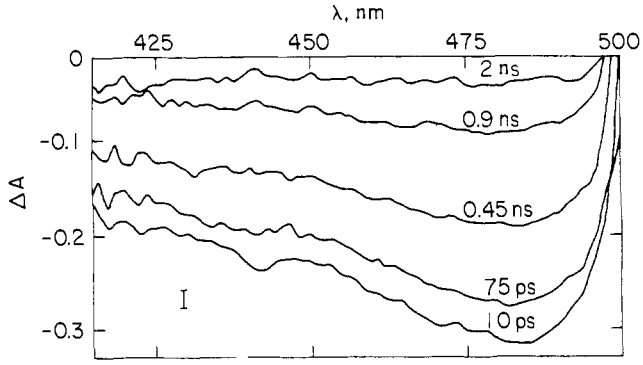

Figure 3. Bleaching of a 2×10^{-4} M solution of $Fe(phen)_3^{2+}$ in a 2-mm path length cell at five different times after excitation with 527-nm light. The data from 480 to 500 nm should be disregarded, because the double monochromator (used to eliminate scattered 527-nm light) did not transmit sufficient probe light in this region to make meaningful absorbance measurements. Typical error is $\pm 0.01 \Delta A$. The ground-state repopulation time is 800 ± 70 ps in the 430-480-nm region.

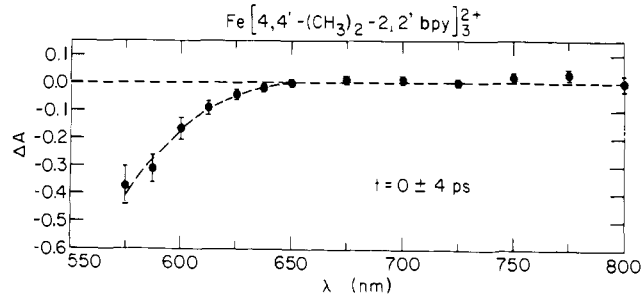

Figure 4. The magnitude of absorbance bleaching for $Fe(4,4'\text{-}(CH_3)_2bpy)_3^{2+}$ at 0 ± 4 ps as a function of wavelength.

A beam splitter was inserted in the continuum beam prior to the sample to create a reference beam.[21-23] The reference beam bypassed the excited sample and was directed into the spectrograph just above the continuum beam that traversed the sample. At the exit slit the two beams were again separated and directed either to different photodiodes (0.75-m Spex monochromator) or to different parts of a vidicon detector (0.25-m J-Y spectrograph). The presence or absence of a mirror after the sample (see dashed lines in Figure 1) determined which detection system was employed. The vidicon detector (SIT tube, Princeton Applied Research OMA-II) could monitor a 320-nm spectral region in a single shot with 2.6-nm resolution (100-μ slits). About 24 pairs of laser shots were averaged for each time point. (A pair consisted of one laser shot with the photolysis pulse blocked and one without blocking; a reference beam was used because the spectral shape of the continuum pulse varied from shot to shot). This procedure resulted in an average scatter in ΔA of about 0.02. The change in the ratio of the light in the two continuum beams following irradiation of the sample with 527-nm light was also measured with a pair of photodiodes. While only a single wavelength (1.7-nm resolution) could be monitored with the photodiodes, there was less error than with the vidicon detector: using an equivalent number of laser shots, an average scatter in ΔA of about 0.005 was obtained with the photodiodes.

The energy of the 527-nm photolysis pulse was about 3-4 mJ at the sample cell (4.5-mm^2 cross-sectional area). After generation in a KDP crystal, the pulse was deflected along a 1-m delay line. By sliding a pair of 45° incident mirrors along a track, delays could be created between the arrival times of the photolysis and continuum pulses at the sample. This meant that absorbance measurements could be made coincident with the photolysis pulse ($t = 0$) and up to 6 ns after it. The experimental uncertainty was about ±4 ps due to the ~8-ps duration of the 1054 pulse.

The FeL_3^{2+} samples were dissolved in water at concentrations of $\sim 6 \times 10^{-4}$ M. The monitoring path length was 2 mm. The samples were shaken after each photolysis shot.

Results

Typical kinetic data for the repopulation of the ground state of FeL_3^{2+} after excitation with a ~6-ps pulse of 527-nm light are shown in Figure 2 for L = terpy and 4,4'-dimethyl-2,2'-bipyridine ($4,4'\text{-}(CH_3)_2bpy$). Bleaching of ground-state absorption resulted from the excitation pulse; then the ground-state absorption was restored exponentially. The same behavior was observed for all of the iron(II) complexes investigated, including $Fe(phen)_3^{2+}$, which was studied in the wavelength range 400-500 nm. See Figure 3. Thus we find no evidence for the 70-ps state of $Fe(phen)_3^{2+}$ reported by Street et al.[10] In fact, we estimate that for all of these iron(II) complexes the nanosecond state is formed quantitatively in <10 ps. The wavelength dependence of the bleaching at 0 ± 4 ps for the $4,4'\text{-}(CH_3)_2bpy$ complex is shown in Figure 4. The lifetimes determined for the iron(II) complexes follow: $Fe(terpy)_2^{2+}$, 2.54 ± 0.13 ns; $Fe(4,4'\text{-}(CH_3)_2bpy)_3^{2+}$, 0.76 ± 0.04 ns; $Fe(bpy)_3^{2+}$, 0.81 ± 0.07 ns; $Fe(phen)_3^{2+}$, 0.80 ± 0.07 ns; $Fe(4,7\text{-}(SO_3C_6H_5)_2\text{-}phen)_3^{4-}$, 0.43 ± 0.03 ns. In Table I, excited-state lifetimes for the OsL_3^{2+} complexes are summarized along with spectral data for the complexes. The lifetimes determined here for the $Os(bpy)_3^{2+}$, $Fe(bpy)_3^{2+}$, and $Fe(phen)_3^{2+}$ excited states, 19 ± 1, 0.81 ± 0.07, and 0.80 ± 0.07 ns, respectively, are in good agreement with those determined by other workers: Lin and Sutin[3] report 19.2 ns for $Os(bpy)_3^{2+}$ under the same conditions, while Kirk et al.[9] find 0.83 ± 0.07 ns for $Fe(bpy)_3^{2+}$ and Street et al. find 0.71 ± 0.05 ns for $Fe(phen)_3^{2+}$.

In Figure 5 difference spectra obtained for $*Os(bpy)_3^{2+}$, $*Fe(bpy)_3^{2+}$, and $*Ru(bpy)_3^{2+}$ are presented. Difference spectra for $*Ru(bpy)_3^{2+}\text{-}Ru(bpy)_3^{2+}$ have also been reported by Bensasson et al.[24] and by Lachish et al.[25] That shown in Figure 5 is in good agreement[26] with the earlier work. In calculating the (absolute) spectra of the excited states the concentrations of the excited states must be known. For $Os(bpy)_3^{2+}$ and $Ru(bpy)_3^{2+}$ the excitation pulses were short compared to the lifetimes of the excited states and eq 2 could be used; the excited-state concentration after the pulse was calculated from the ground-state molar absorptivity and the number of incident 530-nm photons, etc. For $Os(bpy)_3^{2+}$ the excited-state yields calculated from eq 2 were in excellent agreement with observed values of $\Delta A/A_0$ at 480 nm, where $*Os(bpy)_3^{2+}$ absorbs negligibly. As the $*Fe(bpy)_3^{2+}$ lifetime is so short the steady-state concentration of excited state present during a relatively long excitation pulse of intensity I_0 could be calculated from the equation

$$\frac{c^*}{c_0} = \frac{k_1}{k_1 + k_d}[1 - \exp\{-(k_1 + k_d)\Delta t\}] \qquad (3)$$

Table I. Spectral Properties and Lifetimes of Osmium(II) Polypyridine Complexes, OsL_3^{2+} [a]

ligand, L [b]	absorption max (molar absorptivity) λ, nm ($10^{-4}\epsilon$, M^{-1} cm^{-1})	uncor emission max [d] λ, nm	lifetime, ns H_2O	lifetime, ns D_2O
4,4′-$(CH_3)_2$bpy	600 (0.34), 488 (1.2), 455 (1.2), 372 (1.1), 335 (1.1), 288 (15.6), 256 (2.1), 247 (2.3)	735	<10	18
bpy	590 (0.32), 480 (1.2), 435 (1.1), 385 (0.88), 367 (0.93), 330 (0.83), 290 (8.0), 245 (2.5)	715	19 ± 1	
bpy-d_8		713	32	41
5,6-$(CH_3)_2$phen	560 (0.46), 480 (1.6), 435 (1.63), 315 (1.1), 271 (8.7), 241 (6.8), 220 (6.4), 205 (7.3)	705	63	119 ± 5
5-(CH_3)phen	570 (0.40), 480 (1.6), 432 (1.6), 267 (9.5), 236 (5.7), 220 (7.0), 205 (8.0)	700	69	
5-Cl(phen)	560 (0.51), 477 (1.6), 434 (1.7), 266 (9.6), 237 (5.1)	700	78	140 ± 5
phen	560 (0.44), 475 (1.5), 430 (1.6), 315 (0.51), 263 (8.6), 220 (6.9), 203 (7.0)	700	84	
4,4′-$(C_6H_5)_2$bpy [c]	615 (0.55), 510 (1.8), 455 (2.2), 385 (1.8), 355 (2.2), 312 (6.8), 262 (7.5)		52 ± 3 (C_2H_5OH)	
4,7-$(C_6H_5)_2$phen [c]	500 (1.5), 447 (1.8), 280 (8.8)		200 ± 20 (C_2H_5OH)	

[a] In water, 25 °C unless otherwise stated. Absorption spectra and lifetimes determined for solutions 0.2 to 1.0×10^{-4} M; solutions for emission spectra were $\sim 10^{-5}$ M and 480 nm was used as the excitation wavelength. [b] The abbreviations used are as follows: bpy, 2,2′-bipyridine; 4,4′-$(CH_3)_2$bpy, 4,4′-dimethyl-2,2′-bipyridine; bpy-d_8, perdeuterio-2,2′-bipyridine; 5,6-$(CH_3)_2$phen, 5,6-dimethyl-1,10-phenanthroline; 5-(CH_3)phen, 5-methyl-1,10-phenanthroline; 5-Cl(phen), 5-chloro-1,10-phenanthroline; phen, 1,10-phenanthroline; 4,4′-$(C_6H_5)_2$bpy, 4,4′-diphenyl-2,2′-bipyridine; 4,7-$(C_6H_5)_2$phen, 4,7-diphenyl-1,10-phenanthroline. [c] In ethanol, 25 °C. [d] Uncorrected emission spectra, determined in the energy mode on the Perkin-Elmer MPF-4 spectrofluorimeter. In general, the complexes also exhibit a weak, ill-defined shoulder at ~760 nm.

(See Appendix for the derivation of eq 3.) Here k_I is the excitation rate constant, $k_I = \phi^*(2.3 \times 10^3)\epsilon I_0$, ϕ^* is the quantum yield for the formation of the excited state, ϵ_0 is the molar absorptivity of the ground state at the excitation wavelength, k_d is the excited-state deactivation rate constant (the reciprocal of the excited-state lifetime), and Δt is the duration of the approximately rectangular excitation pulse. For $Fe(bpy)_3^{2+}$ $k_d = 1/\tau = 1.2 \times 10^9$ s^{-1} and $\epsilon_{530} = 0.8 \times 10^4$ M^{-1} cm^{-1}. Under the conditions used the pulse length Δt was 22×10^{-9} s and I_0 was typically 2×10^1 einsteins cm^{-2} s^{-1}, so that k_I was 4.6×10^8 s^{-1} (assuming $\phi^* = 1$). The exponential term in eq 3 is thus negligible and the simplified equation

$$\frac{c^*}{c_0} = \frac{k_I}{k_I + k_d} \tag{4}$$

may be used for $*Fe(bpy)_3^{2+}$. In order to verify that this treatment is valid, the magnitude of the bleaching at 500 nm was monitored as a function of excitation intensity for $Fe(bpy)_3^{2+}$. These data are presented in Figure 6 as a plot of $(\Delta A/A_0)^{-1}$ at 500 nm vs. $(I_0)^{-1}$, where I_0 is the relative intensity. It follows from eq 4 that

$$\frac{c_0}{c^*} = 1 + \frac{k_d}{k_I} \tag{5a}$$

or

$$\left(\frac{\Delta A}{A_0}\right)^{-1} = \frac{\epsilon_\lambda}{(\epsilon_\lambda^* - \epsilon_\lambda)} + \frac{\epsilon_\lambda k_d}{(\epsilon_\lambda^* - \epsilon_\lambda)k_I} \tag{5b}$$

where ϵ_λ and ϵ_λ^* are the molar absorptivities of ground and excited states at the monitoring wavelength λ. For Figure 6, the intercept = 0.95 ± 0.08, the slope = 40 ± 10 einsteins cm^{-2} s^{-1}, and slope/intercept = 42 ± 14 einsteins cm^{-2} s^{-1}. The linearity of the plot confirms the applicability of the simplified relation eq 5. The magnitude of the intercept 0.95 indicates that $*Fe(bpy)_3^{2+}$ does not absorb significantly at 500 nm ($\epsilon_{500}^* \leq 5 \times 10^2$ M^{-1} cm^{-1}). Finally, comparison of the observed slope-to-intercept ratio 41 ± 14 einsteins cm^{-2} s^{-1} with the calculated quantity $k_d/(2.3 \times 10^3\epsilon) = 65$ einsteins cm^{-2} s^{-1} obtained for $\epsilon = 0.8 \times 10^4$ M^{-1} cm^{-1}, $k_d = 1.2 \times 10^9$ s^{-1}, gives $\phi^* = 1.6 \pm 0.5$. Thus it is evident that ϕ^* is high and probably unity, within experimental error.

The results of quenching measurements for $*RuL_3^{2+}$, $*OsL_3^{2+}$, and $*FeL_3^{2+}$ are summarized in Table II. In an effort to determine the rate constants for oxidation of $*Fe(bpy)_3^{2+}$ and $*Fe(terpy)_2^{2+}$ by Fe_{aq}^{3+}, 10^{-4} M $Fe(bpy)_3^{2+}$ or $Fe(terpy)_2^{2+}$ was excited in the presence of 0.1 M Fe_{aq}^{3+} (0.5 M H_2SO_4, 25 °C) with a 22-ns pulse of intensity 10^2 einsteins cm^{-2} s^{-1}. At the end of the pulse no ground-state bleaching was observed ($\Delta A_{500} \leq 4 \times 10^{-3}$; $(c_0 - c_1)/c_0 \leq 6 \times 10^{-3}$). From eq 5c, a rate constant of $\leq 1 \times 10^7$ M^{-1} s^{-1} is obtained for the reaction of $*Fe(bpy)_3^{2+}$ or $*Fe(terpy)_2^{2+}$ with Fe^{3+}.

$$\ln\left(\frac{c_0}{c_0 - c_1}\right) = \frac{k_q k_I \Delta t[Fe^{3+}]}{k_I + k_d + k_q[Fe^{3+}]} \tag{5c}$$

Table II. Rate Constants for Quenching of Excited States of Polypyridyl Complexes at 25 °C in Aqueous Solution

donor	quencher	ionic strength, M (medium)	k_q, [a] M^{-1} s^{-1}
$*Ru(bpy)_3^{2+}$	$Os(bpy)_3^{2+}$	0.1 (NaCl)	1.5×10^9
$*Ru(5\text{-Cl-phen})_3^{2+}$	$Os(bpy)_3^{2+}$	1.0 (Na_2SO_4)	2.5×10^9
$*Ru(4,7\text{-}(CH_3)_2\text{-phen})_3^{2+}$	$Os(bpy)_3^{2+}$	1.0 (Na_2SO_4)	2.5×10^9
$*Ru(bpy)_3^{2+}$	$Ru(bpy)_3^{2+}$	1.0 (Na_2SO_4)	$\leq 10^8$
$*Ru(bpy)_3^{2+}$	$Ru(terpy)_2^{2+}$	1.0 (Na_2SO_4)	1.5×10^9
		0.1 (NaCl)	1.2×10^9
$*Ru(bpy)_3^{2+}$	$Ru(5\text{-}NO_2\text{-phen})_3^{2+}$	0.1 (NaCl)	2.0×10^9
$*Ru(bpy)_3^{2+}$	$Ru(TPTZ)_2^{2+}$	0.5 (NaCl)	1.2×10^9
$*Os(5\text{-Clphen})_3^{2+}$	$Ru(terpy)_2^{2+}$	1.0 (Na_2SO_4)	$\leq 1 \times 10^8$
$*Os(5\text{-Clphen})_3^{2+}$	$Ru(TPTZ)_2^{2+}$	0.5 (NaCl)	2.6×10^9
$*Ru(bpy)_3^{2+}$	$Fe(phen)_3^{2+}$	0.1 (NaCl)	1.1×10^9
$*Ru(bpy)_3^{2+}$	$Fe(bpy)_3^{2+}$	0.5 (Na_2SO_4)	1.0×10^9
$*Os(5\text{-Clphen})_3^{2+}$	$Fe(phen)_3^{2+}$	0.5 (NaCl)	1.4×10^9
$*Os(5\text{-Clphen})_3^{2+}$	$Fe(bpy)_3^{2+}$	0.5 (NaCl)	2.3×10^9
$*Os(5\text{-Clphen})_3^{2+}$	$Ru(NH_3)_6^{2+}$	0.5 (NaCl)	1.1×10^9
$*Os(5\text{-Clphen})_3^{2+}$	$Ru(NH_3)_6^{2+}$	0.5 (NaCl)	3.4×10^9
$*Os(5\text{-Clphen})_3^{2+}$	$Fe(CN)_6^{4-}$	1.0 (NaCl)	2.8×10^8
$*Os(5\text{-Clphen})_3^{2+}$	Eu_{aq}^{2+}	0.5 (0.05 H^+, NaCl)	7.9×10^6
$Fe(terpy)_2^{2+}$	Fe_{aq}^{3+}	0.5 (H_2SO_4)	$\leq 4 \times 10^6$
$Fe(bpy)_3^{2+}$	Fe_{aq}^{3+}	0.5 (H_2SO_4)	$\leq 1 \times 10^7$

[a] Error bars are estimated to be ±10% of the rate constant reported here.

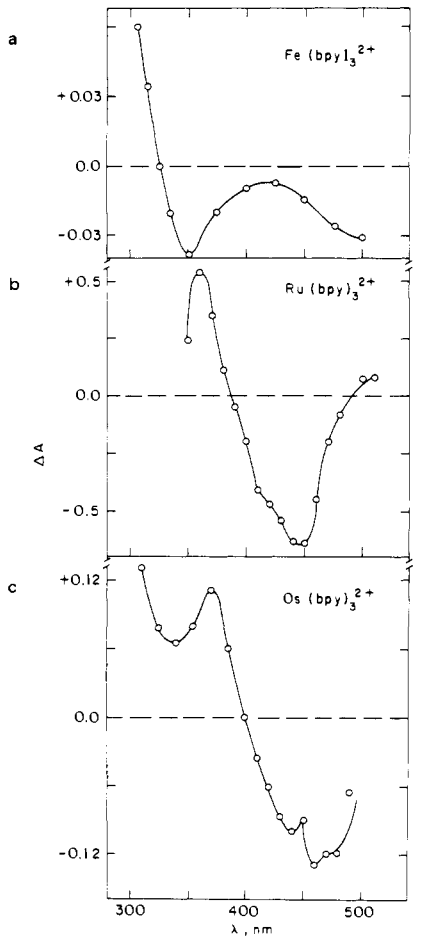

Figure 5. (a) Difference spectrum obtained for $*Fe(bpy)_3^{2+}$ by monitoring maximal absorbance readings during a 20-ns pulse of 530-nm light. (b) Difference spectrum obtained for $*Ru(bpy)_3^{2+}$ with 530-nm excitation (20-ns pulse): 3×10^{-5} M $Ru(bpy)_3^{2+}$, 0.39-cm path length along interrogation beam, 10-nm slit width; the fraction of ground state converted to excited state was ~0.3. (c) Difference spectrum obtained for $*Os(bpy)_3^{2+}$ with 530-nm excitation (8-ns pulse). The aqueous solution was 5×10^{-5} M in $Os(bpy)_3^{2+}$. The path length along the interrogation beam was 0.39 cm; the fraction of ground state converted to excited state was 0.72 ± 0.07.

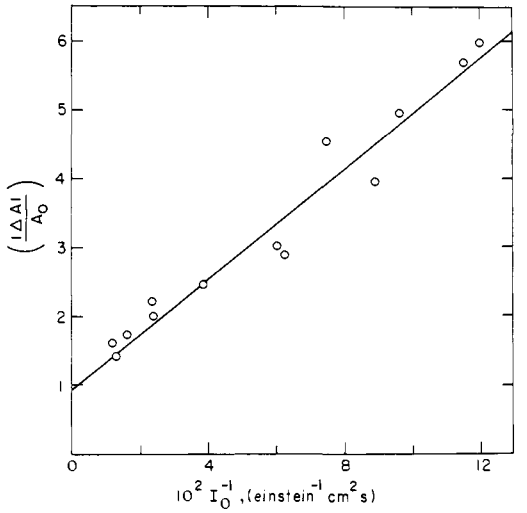

Figure 6. Reciprocal of the fraction of the $Fe(bpy)_3^{2+}$ absorbance bleaching at 500 nm vs. the reciprocal of the excitation intensity.

Table III. Excited-State Lifetimes for Polypyridine Complexes of Chromium(III), Ruthenium(II), Osmium(II), and Iron(II) in Aqueous Solution at 25 °C

	τ			
ligand, L	Cr,[a] μs	Ru,[b] ns	Os,[c] ns	Fe,[d] ns
terpy	0.05	≤5, ≥1.2[e]		2.54 ± 0.13
4,4′-$(CH_3)_2$bpy	156	330	(~9)	0.76 ± 0.04
bpy	66	600	19	0.81 ± 0.07
bpy-d_8	66[f]	690	32	
5,6-$(CH_3)_2$phen		1810	63	
5-(CH_3)phen		1330	69	
4,7-$(CH_3)_2$phen	265	1740		
5-Clphen	134	940	78	
phen	270	920	84	0.80 ± 0.07
4,7-$(SO_3Ph)_2$-phen^{2-}		3860		0.43 ± 0.03

[a] Lifetimes in 1 M HCl, from ref 28. [b] Lifetimes in water. See ref 11. [c] This work. [d] This work, 22–25 °C. [e] Young, R. C.; Nagle, J. K.; Meyer, T. J.; Whitten, D. G.; *J. Am. Chem. Soc.* **1978**, *100*, 4773. [f] Brunschwig, B. S., unpublished observations.

Discussion

The ground-state complexes FeL_3^{2+}, RuL_3^{2+}, and OsL_3^{2+} are all low spin $(t_{2g})^6$. The excited states of RuL_3^{2+} and OsL_3^{2+} are charge transfer in nature and may be crudely described as $(t_{2g})^5(\pi^*)^1$. The nature of the iron(II) excited state(s) investigated here has not, however, been established. Unlike RuL_3^{2+} and OsL_3^{2+}, the FeL_3^{2+} complexes are not luminescent.[8] Kirk et al.,[9] drawing on the spectral assignments of Palmer and Piper,[27] concluded that the 0.8-ns excited state of $Fe(bpy)_3^{2+}$ may be either the triplet charge-transfer excited state or the lowest ligand-field state. Street et al.[10] have proposed that the 0.8-ns state of $Fe(phen)_3^{2+}$ is ligand field in nature. The observations we have described here lead us, as well, to this conclusion. As a working hypothesis, we adopt the model that $*FeL_3^{2+}$ is a ligand-field state—either $^3T_1$ or $^5T_2$—and consider the observed properties of the excited state with those expected to this assignment.

Excited-State Lifetimes. The lifetimes of the excited states of polypyridine complexes of chromium(III), ruthenium(II), osmium(II), and iron(II) in aqueous solutions at room temperature are summarized in Table III. Since these metal complexes emit weakly (if at all) in aqueous solution at ambient temperature, their lifetimes are determined by radiationless decay processes. It is apparent, however, that the factors determining the radiationless decay rates are not the same for all the excited states studied. For the $3d^3$ chromium(III) complexes, the lifetimes determined by Brunschwig and Sutin[28] are for the decay of a ligand-field excited state.[29] As mentioned above, we propose that the excited states of the iron(II) complexes are also ligand field in nature. Consistent with this interpretation it should be noted that the FeL_3^{2+} lifetimes do not parallel the general trends established by the RuL_3^{2+} and OsL_3^{2+} charge-transfer excited states. While the osmium lifetimes are 10–30 times shorter than the ruthenium lifetimes, the lifetimes of the complexes do follow the same rough order: those containing phenanthroline ligands are longer lived than those containing 2,2′-bipyridine ligands. For ruthenium, for which the largest set of data is available, the extremes are found for $Ru(terpy)_2^{2+}$ (shortest) and $Ru(4,7\text{-}(SO_3C_6H_5)_2phen)_3^{4-}$ (longest). The opposite extremes are found for iron; the longest lived iron(II) complex is $Fe(terpy)_2^{2+}$ while the shortest lived is $Fe(4,7\text{-}(SO_3C_6H_5)_2phen)_3^{4-}$. Only limited comparisons between iron(II) and chromium(III) are possible: for chromium the order is τ for L = phen > 4,4′-$(CH_3)_2$bpy > bpy ≫ terpy, but for iron it is terpy > bpy ~ phen > 4,4′-$(CH_3)_2$bpy. The relatively short, ligand-insensitive lifetimes of the FeL_3^{2+} excited states suggest that the radiationless decay of the FeL_3^{2+} complexes differs in at least one important respect from the decay of the RuL_3^{2+}, OsL_3^{2+},

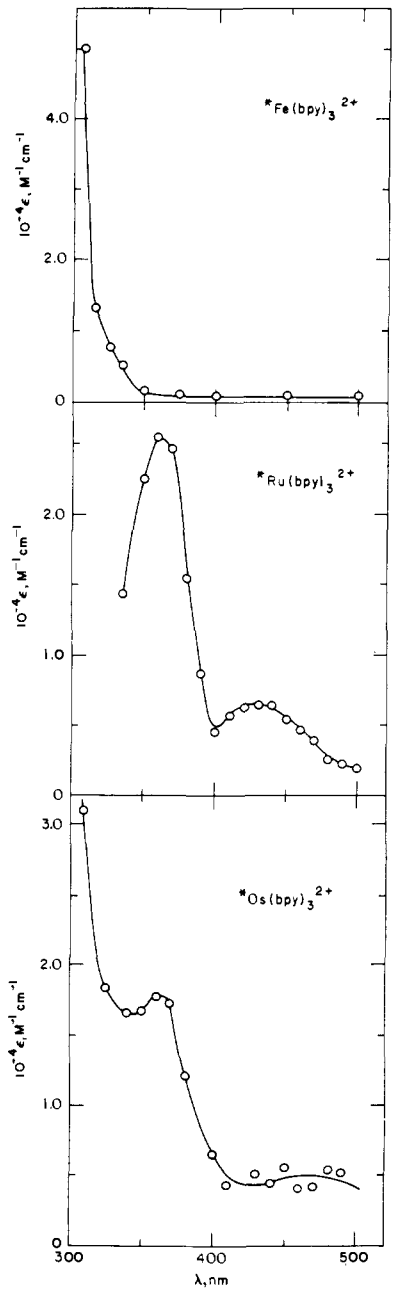

Figure 7. The spectra of $*Fe(bpy)_3^{2+}$, $*Ru(bpy)_3^{2+}$, and $*Os(bpy)_3^{2+}$ based on the data presented in Figure 5.

and CrL_3^{3+} complexes. This difference may have its origin in the geometries of the excited states of the FeL_3^{2+} complexes, unlike those of the other complexes considered, being substantially distorted from the ground-state geometries. This is expected because of the population of the e_g orbitals in the (ligand-field) excited states of the FeL_3^{2+} complexes. As a consequence the ground- and excited-state potential energy surfaces of the FeL_3^{2+} complexes may cross (strong coupling limit) rather than nestle as they do for $*RuL_3^{2+}$ and $*OsL_3^{2+}$ (and the MLCT state of FeL_3^{2+}) and their respective ground states. This could account for the insensitivity of the $*FeL_3^{2+}$ lifetimes to the nature of L: in the strong-coupling limit, excited-state deactivation is determined by the magnitude of inner shell and solvent distortion and by spin-orbit coupling factors which are expected to be similar for the various ligands studied.

Excited-State Spectra. The visible absorption spectra of ground-state $Fe(bpy)_3^{2+}$, $Ru(bpy)_3^{2+}$, and $Os(bpy)_3^{2+}$ are dominated by intense $t_{2g} \rightarrow \pi^*$ metal-to-ligand charge-transfer transitions. The excited-state spectra of these complexes are presented in Figure 7. As was noted previously,[2a] the spectral features of $*Ru(bpy)_3^{2+}$ and $*Os(bpy)_3^{2+}$ are similar and reminiscent of the spectrum of the 2,2′-bipyridine radical anion reported by Mahon and Reynolds.[30] For $*Ru(bpy)_3^{2+}$ and $*Os(bpy)_3^{2+}$, two maxima are seen. These occur at ~360 and at 430 or 460 nm, respectively, and may correspond to the radical anion peaks at 386 and 420 nm. The spectral features of these excited states are thus consistent with the ligand-localized transitions of a $(t_{2g})^5(\pi^*)^1$ metal-to-ligand charge-transfer excited state. On the other hand, the spectrum of $*Fe(bpy)_3^{2+}$ is featureless above ~300 nm. Intense absorption is seen below 300 nm, but no absorption maxima are found between 270 and 510 nm. This striking contrast between the spectra of $*Fe(bpy)_3^{2+}$ on the one hand and of $*Os(bpy)_3^{2+}$, $*Ru(bpy)_3^{2+}$, and bpy^- on the other suggests that $*Fe(bpy)_3^{2+}$ does not possess the bipyridine anion chromophore, i.e., that $*Fe(bpy)_3^{2+}$ is not a metal-to-ligand charge-transfer excited state. This conclusion is consistent with the assignment made above, namely, that $*Fe(bpy)_3^{2+}$ is a ligand-field state, either $^3T_1$ or $^5T_2$. The spectral features of either state would include ligand localized transitions (π-π^* around 290 nm as observed for $Fe(bpy)_3^{2+}$, etc.), weak ligand-field transitions of the metal center, and weak metal-to-ligand charge-transfer transitions in the visible. In particular, neither state is likely to exhibit intense low-energy metal-to-ligand charge transfer as is seen for $Fe(bpy)_3^{2+}$ in the visible.[31-33]

Quenching Rate Constants. Three processes must be considered as possible quenching pathways for the polypyridine excited states:

$$*ML_3^{2+} + Q \rightarrow ML_3^{3+} + Q^- \quad (6)$$

$$*ML_3^{2+} + Q \rightarrow ML_3^{+} + Q^+ \quad (7)$$

$$*ML_3^{2+} + Q \rightarrow ML_3^{2+} + Q^* \quad (8)$$

The first two, eq 6 and 7, involve respectively oxidation and reduction of the $*ML_3^{2+}$ excited state, while in eq 8 electronic excitation is transferred by an energy-transfer process to Q. These three quenching processes may proceed in parallel so that the observed quenching rate constant may contain contributions from all three:

$$k_{q,obsd} = k_6 + k_7 + k_8$$

Despite this complication it is possible to deduce the major quenching mechanism in a number of the systems studied. As the electron-transfer quenching reactions are expected to be a function of the oxidation-reduction potentials of the reactants, while energy-transfer processes should depend on spectral overlap considerations, the reduction potentials and spectral data of the polypyridine complexes used in this study are summarized in Table IV and will be used as a basis for discussion in the following paragraphs.

Electron-Transfer Quenching. Models and information amassed for ground-state reactions provide a useful guide for the excited-state electron-transfer reactions, eq 6 and 7. Ground-state outer-sphere electron-transfer reactions of $FeL_3^{2+/3+}$, $RuL_3^{2+/3+}$, and $OsL_3^{2+/3+}$ are very rapid. This is attributed to the low intrinsic barriers to electron transfer that obtain in this series and which are most evident in the self-exchange process:

$$ML_3^{2+} + ML_3^{3+} \rightleftharpoons ML_3^{3+} + ML_3^{2+} \qquad k_{ex} \quad (9)$$

Rate constants of 5×10^7 to 1×10^9 M^{-1} s^{-1} in water at 25 °C have been determined for reaction 9.[34,35] In addition there is compelling evidence that the couples involving the charge-transfer excited states of RuL_3^{2+} and OsL_3^{2+} also possess very high self-exchange rates (eq 10 and 11); rate constants of $\geq 10^8$ and 10^9 M^{-1} s^{-1} have been estimated for the excited-state

Table IV. Reduction Potentials and Absorption and Emission Maxima for Polypyridine Complexes of Iron(II), Ruthenium(II), and Osmium(II) at 25 °C[a]

complex	ground state[a] $E°_{3,2}$, V	ground state[a] $E°_{2,1}$, V	excited state[a] $*E°_{3,2}$, V	excited state[a] $*E°_{2,1}$, V	absorption[b] λ_{max}, nm	emission[b] λ_{max}, nm
$Ru(bpy)_3^{2+}$	+1.26	−1.28	−0.84	+0.84	452, 560	613, 627
$Ru(5\text{-}Clphen)_3^{2+}$	+1.36	−1.15	−0.77	+1.00	422, 447, (560)[f]	605, 625
$Ru(4,7\text{-}(CH_3)_2phen)_3^{2+}$	+1.09	−1.47	−0.94	+0.67	425, 445, (560)[f]	613, 627
$Ru(terpy)_2^{2+}$	+1.25	−1.36			473 (560)	628
$Ru(5\text{-}NO_2phen)_3^{2+}$	+1.46[b]		−0.67[b]		449 (560)	606
$Ru(TPTZ)_2^{2+}$	+1.49	−0.77			501 (560)	605
$Os(bpy)_3^{2+}$	+0.82	−1.22	−0.96	+0.59	480, 590, 650	750[d]
$Os(5\text{-}Clphen)_3^{2+}$	+0.93	−1.09	−0.9	+0.7	477, 560, (650)[f]	700[e]
$Fe(phen)_3^{2+}$	+1.06[b]				510[g]	
$Fe(bpy)_3^{2+}$	+1.05[b]	−1.26[i]			522,[g] 870[h]	
$Fe(terpy)_2^{2+}$	+1.05[c]	−1.17[i]			522[g]	

[a] Data taken from Tables II and III of ref 2a unless otherwise stated. See ref 2a for original literature references. [b] From ref 15 unless otherwise noted. See ref 15 for original literature reference. Unless otherwise noted, *corrected* emission maxima are reported. [c] Dwyer, F. P.; Gyarfas, E. C. *J. Am. Chem. Soc.* **1954**, *76*, 6320. [d] Reference 3. [e] Uncorrected emission maximum. [f] Assumed by analogy with the spectrum of $M(bpy)_3^{2+}$. See text. [g] Reference 14. [h] Reference 27. [i] Saji, T.; Aoyagui, S. *J. Electroanal. Chem. Interfacial Electrochem.* **1975**, *58*, 401.

Table V. Quenching Mechanisms for Polypyridine Complexes

	reactants: donor	reactants: quencher	$-\Delta E°_{el,6}$, V	$-\Delta E°_{el,7}$, V	$\Delta E*$, eV	k_q, $M^{-1}\,s^{-1}$	probable reaction	postulated products
1.	$*Ru(bpy)_3^{2+}$	$Os(bpy)_3^{2+}$	+0.38	−0.02	−0.33	1.5×10^9	7	$Ru(bpy)_3^{+} + Os(bpy)_3^{3+}$
							8	$Ru(bpy)_3^{2+} + *Os(bpy)_3^{2+}$
2.	$*Ru(5\text{-}Clphen)_3^{2+}$	$Os(bpy)_3^{2+}$	+0.45	−0.18	−0.33	2.5×10^9	7	$Ru(5\text{-}Clphen)_3^{+} + Os(bpy)_3^{3+}$
							8	$Ru(5\text{-}Clphen)_3^{2+} + *Os(bpy)_3^{2+}$
3.	$*Ru(4,7\text{-}(CH_3)_2\text{-}phen)_3^{2+}$	$Os(bpy)_3^{2+}$	+0.28	+0.15	−0.33	2.5×10^9	8	$Ru(4,7(CH_3)_2phen)_3^{2+} + *Os(bpy)_3^{2+}$
4.	$*Ru(bpy)_3^{2+}$	$Ru(bpy)_3^{2+}$	+0.44	+0.41	~0	$<1 \times 10^8$	none	none
5.	$*Ru(bpy)_3^{2+}$	$Ru(terpy)_2^{2+}$	+0.52	+0.35	~0	1.5×10^9	8	$Ru(bpy)_3^{2+} + *Ru(terpy)_3^{2+}$
6.	$*Ru(bpy)_3^{2+}$	$Ru(5\text{-}NO_2\text{-}phen)_3^{2+}$		+0.62	~0	2.0×10^9	(6)	$Ru(bpy)_3^{3+} + Ru(5\text{-}NO_2)phen)_3^{+}$
							8	$Ru(bpy)_3^{2+} + *Ru(5\text{-}NO_2)\text{-}phen)_3^{2+}$
7.	$*Ru(bpy)_3^{2+}$	$Ru(TPTZ)_2^{2+}$	−0.07	+0.65	~0	1.2×10^9	6	$Ru(bpy)_3^{3+} + Ru(TPTZ)_2^{+}$
							8	$Ru(bpy)_3^{2+} + *Ru(TPTZ)_2^{2+}$
8.	$*Os(5\text{-}Clphen)_3^{2+}$	$Ru(terpy)_2^{2+}$	+0.5	+0.6	+0.33	$<1 \times 10^8$	none	none
9.	$*Os(5\text{-}Clphen)_3^{2+}$	$Ru(TPTZ)_2^{2+}$	−0.1	+0.8	+0.33	2.6×10^9	6	$Os(5\text{-}Clphen)_3^{3+} + Ru(TPTZ)_2^{+}$
10.	$*Ru(bpy)_3^{2+}$	$Fe(phen)_3^{2+}$		+0.22		1.1×10^9	(6)	$Ru(bpy)_3^{3+} + Fe(phen)_3^{+}$
							8	$Ru(bpy)_3^{2+} + *Fe(phen)_3^{2+}$
11.	$*Ru(bpy)_3^{2+}$	$Fe(bpy)_3^{2+}$	+0.42	+0.21		1.0×10^9	8	$Ru(bpy)_3^{2+} + *Fe(bpy)_3^{2+}$
12.	$*Os(5\text{-}Clphen)_3^{2+}$	$Fe(phen)_3^{2+}$		+0.4		1.4×10^9	(6)	$Os(5\text{-}Clphen)_3^{3+} + Fe(phen)_3^{+}$
							8	$Os(5\text{-}Clphen)_3^{2+} + *Fe(phen)_3^{2+}$
13.	$*Os(5\text{-}Clphen)_3^{2+}$	$Fe(bpy)_3^{2+}$	+0.4	+0.4		2.3×10^9	8	$Os(5\text{-}Clphen)_3^{2+} + *Fe(bpy)_3^{2+}$

exchange processes (10) and (11), respectively.[2] Furthermore, the work of Saji and Aoyagui[36] implicates a rate constant of $\geq 10^8$ M^{-1} s^{-1} for eq 12. Finally, both the ground-state and

$$*ML_3^{2+} + ML_3^{3+} \rightleftharpoons ML_3^{3+} + *ML_3^{2+} \quad (10)$$

$$ML_3^{+} + *ML_3^{2+} \rightleftharpoons *ML_3^{2+} + ML_3^{+} \quad (11)$$

$$ML_3^{+} + ML_3^{2+} \rightleftharpoons ML_3^{2+} + ML_3^{+} \quad (12)$$

excited-state reactions respond to reaction driving force (K_{12}) in a way which at moderate driving force is given by the Marcus equation, $\log k_{12} = 0.5 \log k_{11}k_{22}K_{12}$.[37] Here k_{11} and k_{22} are the self-exchange rates of the reactant couples (eq 9–12) and k_{12} is the rate constant for the cross reaction (eq 6 or 7). It becomes evident that reactions 7 and 8 should be very rapid indeed when Q is a polypyridine complex of iron, ruthenium, or osmium provided that $K \geq 1$. From these considerations, it is concluded that for oxidative quenching k_6 should be $\sim 3 \times 10^8$ M^{-1} s^{-1} if $K = 1$ and, in general, k_6 should be $\sim 3 \times 10^8$ $(K^{1/2})$ M^{-1} s^{-1} where K may be calculated from $\Delta E°_{el,6} = E°_{2,1;q} - *E°_{3,2;d}$. Similarly, for reductive quenching, k_7 should be $\sim 3 \times 10^8 (K^{1/2})$ M^{-1} s^{-1} where K is obtained from $\Delta E°_{el,7} = *E°_{2,1;d} - E°_{3,2;q}$. Both electron-transfer processes should approach diffusion-controlled rates ($\sim 3 \times 10^9$ M^{-1} s^{-1}) when $K \geq 10^2$ or $\Delta E° \geq 0.12$ V.

In Table V the data for quenching by polypyridine complexes have been organized so that these predictions can be systematically examined. The third and fourth columns contain values of $\Delta E°$ for quenching according to eq 6 and 7, respectively. Values observed for k_q are given in the penultimate column. For reactants 1, 2, 6, 7, 9, 10, and 12 in Table V $\Delta E°$ is ≥ 0 V for one or the other of the electron-transfer quenching reactions and, notably, all these reactions proceed with quenching rate constants $\geq 10^9$ M^{-1} s^{-1}. Furthermore, for systems 4 and 8 for which K_{12} for quenching by either eq 6 or 7 is less than 10^{-5}, the quenching rate constants are less than 10^8 M^{-1} s^{-1}.

Energy-Transfer Quenching. The reactivity patterns examined so far generally support the rate criteria for electron-transfer quenching developed above. We consider now the rate patterns expected for energy-transfer processes. Within the Dexter model for energy transfer, the efficiency of the transfer increases as spectral overlap between donor and acceptor increases.[38] For the donor, the maximum and shape of the emission band returning the donor to the ground state are considered; for the acceptor, the absorption spectrum is of relevance. With $*RuL_3^{2+}$ and $*OsL_3^{2+}$ as donors, the emission spectra maximize at ~600–630 and at ~750 nm, respectively, and the excited-state energies are estimated to be 16.9 and 14.4

$\times 10^3$ cm^{-1}, respectively. The properties of the potential acceptors RuL_3^{2+} and OsL_3^{2+} will be considered in turn. The principal low-energy absorption features for the Ru(II) complexes (Table IV) are the intense, charge-transfer transitions in the range 420–470 nm, but a weak, spin-forbidden transition has been recognized for $Ru(bpy)_3^{2+}$ at ~590 nm. The latter is the lowest energy absorption band detected and is the counterpart of the emission band at 600–630 nm. The osmium(II) complexes also undergo intense charge-transfer absorption at ~480 nm with a secondary fairly intense band at ~560 nm. In addition, weaker absorption is seen at ~650 nm,[6] a band which probably corresponds to the inverse of the 750-nm emission.

We now consider donor/quencher pairs to determine for which the Dexter criteria for energy transfer are met.

(1) $*RuL_3^{2+}/OsL_3^{2+}$. The Ru(II) emission spectra (λ_{max} 600–630 nm) overlap the absorption spectra of the Os(II) complexes (λ_{max} 590, 650 nm) so that energy transfer from $*RuL_3^{2+}$ to OsL_3^{2+} is generally to be expected. Quenching is thus likely to proceed by energy transfer in systems 1–3 in Table V. In systems 1 and 2 electron-transfer quenching (eq 7) is also expected to be rapid, so that the high values of the quenching rate constants are not readily interpreted. For system 3, however, redox quenching is thermodynamically unfavorable as it is in system 4 for which $k_q \leq 10^8$ M^{-1} s^{-1}. Therefore the high value of $k_q = 2.5 \times 10^9$ M^{-1} s^{-1} with $*Ru(4,7\text{-}(CH_3)_2phen)_3^{2+}/Os(bpy)_3^{2+}$ is ascribed to rapid energy transfer. This is an important conclusion: "thermodynamically favorable" energy transfer from $*RuL_3^{2+}$ to OsL_3^{2+} occurs with a rate constant approaching the diffusion-controlled value.

(2) $*RuL_3^{2+}/RuL_3^{2+}$. By contrast, energy transfer from the excited state of one RuL_3^{2+} complex to the ground state of another is not likely to be very favorable thermodynamically, but rather "thermoneutral". In the RuL_3^{2+} series the absorption and emission spectra (and thus the excited-state energies) are remarkably insensitive to the nature of L.[15] Consequently energy transfer from one RuL_3^{2+} complex to another is rather analogous to the self-exchange process for electron transfer, except that it formally involves *two* simultaneous electron transfers. The data for entries 4–7 bear on this question. For systems 6 and 7 electron-transfer quenching may occur in parallel with energy transfer. It is, however, evident from system 5 ($*Ru(bpy)_3^{2+}/Ru(terpy)_2^{2+}$), for which electron-transfer quenching is highly unfavorable, but $k_q = 1.5 \times 10^9$ M^{-1} s^{-1}, that energy transfer may also be very rapid between various ruthenium(II) complexes. Entry 4, $Ru(bpy)_3^{2+}$ "self-quenching", is an interesting case in point: according to our arguments, "exchange" energy-transfer quenching could also be facile here. However, since each such quenching act must regenerate an excited molecule (eq 13), no net diminution in donor concentration and lifetime can result.

$$*Ru(bpy)_3^{2+} + Ru(bpy)_3^{2+} \rightarrow Ru(bpy)_3^{2+} + *Ru(bpy)_3^{2+} \quad (13)$$

(3) $*OsL_3^{2+}/RuL_3^{2+}$. The absorption spectrum of RuL_3^{2+} does not detectably overlap OsL_3^{2+} emission. Often such an observation is of no great value in predicting energy-transfer efficiencies because energy transfer may occur via acceptor states which are spectroscopically unobserved—for example, via spin-forbidden transitions. In the present case, however, the fact that RuL_3^{2+} emission from the lowest excited state occurs at ~600–630 nm, while the OsL_3^{2+} emission lies at ~750 nm, indicates that the relevant spectral overlap must be poor, largely because the Os(II) complexes have lower excited state energies than the Ru(II) excited states. In other words, energy transfer from $*OsL_3^{2+}$ to RuL_3^{2+} is energetically uphill. Rates for this process are thus expected to be slower than for those discussed above. The validity of this conclusion is supported by the data for system 8, $*Os(5\text{-}Clphen)_3^{2+}/Ru(terpy)_2^{2+}$, for which both electron-transfer and energy-transfer quenching are unfavorable processes; here k_q is $\leq 10^8$ M^{-1} s^{-1}.

Quenching by Polypyridine Iron(II) Complexes. Analysis of the quenching rate patterns for RuL_3^{2+} and OsL_3^{2+} has led to two conclusions: when electron-transfer quenching is thermodynamically favorable, very rapid quenching rate constants (10^9 M^{-1} s^{-1} or greater) are seen. Similarly if energy-transfer quenching is "thermodynamically favorable" ($*E_a < *E_d$), energy-transfer quenching is very rapid. Conversely, when either process is uphill, k_q is diminished ($\leq 10^8$ M^{-1} s^{-1}). For entries 10–13 in Table V, $Fe(bpy)_3^{2+}$ and $Fe(phen)_3^{2+}$ were used as quenchers for $*Ru(bpy)_3^{2+}$ and $*Os(5\text{-}Clphen)_3^{2+}$. In entries 11 and 13 electron-transfer quenching is unfavorable by at least 0.2 V. The rapid quenching observed ($k_q \geq 1 \times 10^9$ M^{-1} s^{-1}) is thus very likely due to energy transfer. The lowest absorption feature observed for $Fe(bpy)_3^{2+}$ is a weak ($\epsilon \sim 1$ M^{-1} cm^{-1}), broad band at ~870 nm. As discussed by Palmer and Piper,[27] this band is probably the ligand-field transition $^1A \rightarrow {}^3T_1$; the three related transitions $^1A \rightarrow {}^1T_1$, $^1A \rightarrow {}^3T_2$, and $^1A \rightarrow {}^1T_2$ must then lie at higher energy, that is, at wavelengths shorter than 870 nm. (The highly forbidden (and therefore very weak) transition $^1A_1 \rightarrow {}^5T_2$ may occur at higher or lower energy than $^1A_1 \rightarrow {}^3T_1$, but should, in any case, occur at lower energy than $^1A \rightarrow {}^3T_2$ or $^1T_1$.) The principal visible absorption feature for $Fe(bpy)_3^{2+}$ is the metal-to-ligand charge-transfer absorption at 522 nm. Presumably the spin-forbidden counterpart of this band lies at longer wavelength. For energy-transfer from $*Ru(bpy)_3^{2+}$ to $Fe(bpy)_3^{2+}$ overlap of $Fe(bpy)_3^{2+}$ absorption with the 630-nm emission of $*Ru(bpy)_3^{2+}$ is required; with $*Os(5\text{-}Clphen)_3^{2+}$ as donor $Fe(bpy)_3^{2+}$ absorption at ~750 nm is needed. Although no such absorptions are observed in the $Fe(bpy)_3^{2+}$ spectrum, it has been inferred that several unobserved spin- or symmetry-forbidden transitions are present between 522 and 870 nm. These may provide acceptor states through which energy transfer from the ruthenium(II) and osmium(II) donors takes place.

Properties of $*FeL_3^{2+}$. The spectrum and lifetime of $*Fe(bpy)_3^{2+}$, the nanosecond state achieved by 530-nm excitation, support its assignment as a ligand-field state. From spectroscopic considerations the lowest ligand-field state of $Fe(bpy)_3^{2+}$ lies at or below 11.5×10^3 cm^{-1} (1.43 eV) and is either $^3T_1$ or $^5T_2$.[27] We postulate that $*Fe(bpy)_3^{2+}$ is $^3T_1$ or $^5T_2$, if the latter is the lowest energy state, and that the excited-state energy is consequently <1.4 eV. From the picosecond experiments $*FeL_3^{2+}$ is formed within ~10 ps after excitation. Thus internal conversion and intersystem crossing to reach the nanosecond state must occur with an overall rate constant of at least $\sim 10^{11}$ s^{-1}. Assuming the initially populated MLCT state to be a singlet, formation of $^3T_1$ or $^5T_2$ states involves a net spin change of 1 or 2, respectively. Rate constants $> 10^7$ s^{-1} have been reported for intersystem crossing between iron(II) ^1A and ^5T ligand-field states of comparable energy.[39] In the present case the intersystem crossings postulated are to states of much lower energy. Since the potential energy surfaces for the MLCT and $^3T_1$ or $^5T_2$ states cross[40] (strong coupling), the rate of intersystem crossing should be enhanced by the fact that the ligand-field states are at lower energy than the MLCT state. Consequently, the intersystem crossing rate should exceed 10^7 s^{-1} and could be as great as 10^{11} s^{-1}. Thus it is not unreasonable that $^3T_1$ or $^5T_2$ be the nanosecond state of $Fe(bpy)_3^{2+}$

The ligand-field states $^3T_1$ and $^5T_2$ have the configurations $(t_{2g})^5(e_g)^1$ and $(t_{2g})^4(e_g)^2$, respectively. Because the antibonding e_g orbitals are populated, the metal–ligand bonds in these states are likely to be ~0.14 Å longer than in the $(t_{2g})^6$

ground state.[39,41] As a consequence of this distortion, the thermally equilibrated $^3T_1$ and $^5T_2$ states should lie ~0.5 eV[42] below the Franck-Condon states. On this basis the thermally equilibrated $^3T_1$ (or $^5T_2$) state is not expected to lie more than ~0.9 eV above the ground state. In summary, an excitation energy of ≤0.9 eV is postulated for $*Fe(bpy)_3^{2+}$. Combining this estimate with the reduction potential of $Fe(bpy)_3^{3+}$ (1.05 V, 0.5 M H_2SO_4[43,15]), $*E°_{3,2}$, the reduction potential of the excited-state couple (eq 14), is ≥ +0.1 V.

$$Fe(bpy)_3^{3+} + e \rightleftharpoons *Fe(bpy)_3^{2+} \quad (14)$$

Because of the distortion of $*Fe(bpy)_3^{2+}$ relative to the ground state, the self-exchange rate of the excited state $*Fe(bpy)_3^{2+}$-$Fe(bpy)_3^{3+}$ couple is expected to be relatively slow. The exchange rate of the ground state $Fe(bpy)_3^{2+}$-$Fe(bpy)_3^{3+}$ couple is $\sim 2 \times 10^9$ M^{-1} s^{-1} [35] and is consistent with essentially zero inner-sphere difference between $Fe(bpy)_3^{2+}$ and $Fe(bpy)_3^{3+}$.[44] The ~0.5-eV distortion[41] of $*Fe(bpy)_3^{2+}$ relative to $Fe(bpy)_3^{2+}$ will contribute ~0.36 eV[47] to the activation energy for the $*Fe(bpy)_3^{2+}$-$Fe(bpy)_3^{3+}$ exchange reaction. On this basis the rate constant for the $*Fe(bpy)_3^{2+}$-$Fe(bpy)_3^{3+}$ exchange reaction is calculated to be $<10^3$ M^{-1} s^{-1}. This exchange rate together with the value of the excited-state potential may be used to calculate a rate constant for the reaction of $*Fe(bpy)_3^{2+}$ (or $*Fe(terpy)_2^{2+}$) with Fe_{aq}^{3+}. From substitution in the Marcus equations[37] we calculate a rate constant for the $*Fe(bpy)_3^{2+}$-Fe_{aq}^{3+} reaction of $<10^6$ M^{-1} s^{-1} which is consistent with the observed value $\leq 10^7$ M^{-1} s^{-1}.[48]

In this study we have presented evidence that, in water at 25 °C, the excited state of $Fe(bpy)_3^{2+}$ arising from 530-nm light absorption undergoes oxidation only rather slowly. There are, however, two reports which appear to conflict with these conclusions. Phillips, Koningstein, Langford, and Sasseville describe electrochemical evidence for photooxidation of $Fe(bpy)_3^{2+}$ by Fe_{aq}^{3+}.[12] Using exciting light in the range 459–514 nm they determined photocurrents at an SnO_2 electrode and deduced a 33-ns lifetime for the $Fe(bpy)_3^{2+}$ excited state and a rate constant of 2.4×10^9 M^{-1} s^{-1} for its oxidation by Fe_{aq}^{3+}. The present studies and those of Kirk et al.[9] (in which ground-state bleaching produced by a subnanosecond pulse of 530-nm light was monitored) provide no evidence for the population of such a long-lived state. Although the excitation wavelength ranges for the electrochemical experiments and the laser excitation experiments do not overlap, it would be quite remarkable if the state produced by the shorter wavelength light did not rapidly convert to that produced by 530-nm excitation. It is more likely that the photocurrents reported arose from species adsorbed on the SnO_2 or from some interfacial artifact. The operation of such effects on SnO_2 is also suggested by the failure of Ohsawa, Saji, and Aoyagui[49] to observe photocurrents at a platinum electrode when $Fe(bpy)_3^{2+}$ was irradiated in the presence of Fe_{aq}^{3+}.

The photooxidation experiments of Chum, Koran, and Osteryoung[11] were carried out in a (nonaqueous) aluminum chloride-ethylpyridinium bromide melt. Both the excited-state lifetimes and the nature of the lowest excited state could change on going from aqueous solution to this medium. If, however, this is not the case, and the active state is a ligand-field state that has a lifetime of ~1 ns, some conclusions may be drawn. The quantum yield for photooxidation of $Fe(bpy)_3^{2+}$ and $Fe(phen)_3^{2+}$ is said to be ~1. If the oxidation involves diffusion of oxidant to $*FeL_3^{2+}$, the rate constant for oxidation must be $\geq 3 \times 10^9$ M^{-1} s^{-1} for such a high quantum yield to obtain, assuming that the oxidant is the 3.2 M ethylpyridinium cation ($Etpy^+$). Such a high oxidation rate constant is not consistent with the oxidation-reduction properties of $*FeL_3^{2+}$ determined in the present study. Thus either the ligand-field state is not active in the nonaqueous melt or a diffusional process is not involved (or, possibly, both). In fact, even if the reaction occurs by "static quenching", the ligand-field state cannot be the active state unless its energy and reactivity are drastically altered by association with $Etpy^+$ (exciplex). Thus it is tempting to propose that associated $Etpy^+$ intercepts a higher excited state of $Fe(bpy)_3^{2+}$ (perhaps indeed the MLCT state as implied by Chum et al.). This process would, however, have to be exceedingly rapid—as much as 10^{11} s^{-1}—since the rate of formation of $Fe(bpy)_3^{2+}$ from the MLCT state (in water) is of this order. Clearly, it is not possible to draw any firm conclusions without further studies of this system.

We have concluded that $*Fe(bpy)_3^{2+}$ is a ligand-field rather than a charge-transfer excited state. This assignment seems reasonable in view of the fact that the ligand-field splitting for iron(II) is relatively small ($10–14 \times 10^3$ cm^{-1},[31] compared to $20–30 \times 10^3$ cm^{-1} for Ru(II)[31] and $>20 \times 10^3$ cm^{-1} for Os(II)). No photoaquation has been reported for $Fe(bpy)_3^{2+}$ or related complexes. In general oxidation-reductions of $*FeL_3^{2+}$ are expected to be rather slow. Consequently, because the lifetimes of these excited states are short, photoinduced electron transfer in FeL_3^{2+} systems may be expected only when the electron acceptor is highly reactive and present in high concentration. In summary, the excited states of FeL_3^{2+} complexes are much less reactive than $*RuL_3^{2+}$ and $*OsL_3^{2+}$ both because of their lower excitation energy (~0.9 vs. 2.1 and 1.8 eV for RuL_3^{2+} and OsL_3^{2+}, respectively) and because their electronic configuration creates high kinetic barriers to electron transfer.

Acknowledgment. Helpful discussions with Drs. Bruce S. Brunschwig, Marshall D. Newton, and Gil Navon are acknowledged. This work was performed under the auspices of the U.S. Department of Energy and supported by its Office of Basic Energy Sciences.

Appendix

By analogy with other scattering processes, a cross section for the interaction of a molecule with an impinging photon may be defined by

$$dI = \sigma N_A c l I_0 / 10^3 \quad (A1)$$

where σ is the molecular cross section (cm^2 $molecule^{-1}$), N_A is Avogadro's number, I_0 is the incident photon intensity (einstein cm^{-2} s^{-1}), dI is the decrease in the photon intensity, c is the concentration of absorbing molecules (mol L^{-1}) and l is the path length of the solution (cm) along the excitation beam. The relation between σ and the usual molar absorptivity (L mol^{-1} cm^{-1}) is given by

$$\sigma N_A / 10^3 = 2.303\epsilon \quad (A2)$$

Substitution of eq A2 into eq A1 gives

$$dI = 2.303\epsilon c l I_0 \quad (A3)$$

which is Beer's law for a dilute solution ($dI \ll I_0$). The number of moles of photons dN absorbed in time dt per unit area of solution is given by

$$dN = 2.303\epsilon c l I_0 \, dt \quad (A4)$$

It follows that the concentration of excited molecules (mol L^{-1}) produced in time dt is given by

$$dc^* = \frac{2.303\epsilon c l I_0 \, dt}{10^{-3} l}$$

The rate of formation of excited molecules is therefore

$$dc^*/dt = 2.303 \times 10^3 \epsilon c I_0 \quad (A5)$$

Provided that I_0 is independent of t, eq A5 may be integrated to give

$$c^* = c_0[1 - e^{-2.303\times10^3\epsilon I_0\Delta t}] \quad \text{(A6)}$$

or

$$c = c_0 e^{-2.303\times10^3\epsilon I_0\Delta t} \quad \text{(A7)}$$

where Δt is the duration of the laser pulse. Inspection of eq A5–A7 shows that we may define a first-order rate constant for the formation of the excited state as follows:

$$k_1 = 2.303 \times 10^3 \epsilon I_0 \quad \text{(A8)}$$

(In molecular cross-section terms, $k_1 = \sigma N_0$ where N_0 is the incident intensity in photons $cm^{-2}\ s^{-1}$). Using this definition of an excitation rate constant, rate equations can be derived that are entirely analogous to the expressions used in conventional kinetic schemes. For example, the above approach can be used to calculate the concentrations of A, B, and C present at the end of a rectangular laser pulse of duration Δt in the two-step scheme

$$A \underset{k_d}{\overset{k_1}{\rightleftharpoons}} B \xrightarrow{k_3} C \quad \text{(A9)}$$

Thus the following rate equations describe the above situation.

$$\begin{aligned} d(A)/dt &= -k_1(A) + k_d(B) \\ d(B)/dt &= k_1(A) - (k_d + k_3)(B) \\ d(C)/dt &= k_3(B) \end{aligned} \quad \text{(A10)}$$

The solution of these equations for the concentrations of the species present at the end of the laser pulse are

$$(A) = (A)_0\left[\frac{k_1 - \lambda_2}{\lambda_1 - \lambda_2} e^{-\lambda_1\Delta t} + \frac{\lambda_1 - k_1}{\lambda_1 - \lambda_2} e^{-\lambda_2\Delta t}\right] \quad \text{(A11)}$$

$$(B) = (A)_0\left[\frac{k_1}{\lambda_1 - \lambda_2}(e^{-\lambda_2\Delta t} - e^{-\lambda_1\Delta t})\right] \quad \text{(A12)}$$

$$(C) = (A)_0\left[[1 + \frac{\lambda_2}{\lambda_1 - \lambda_2} e^{-\lambda_1\Delta t} - \frac{\lambda_1}{\lambda_1 - \lambda_2} e^{-\lambda_2\Delta t}\right] \quad \text{(A13)}$$

where $\lambda_1 = (p + q)/2$; $\lambda_2 = (p - q)/2$; $p = (k_1 + k_d + k_3)$; $q = (p^2 - 4k_1k_3)^{1/2}$. Certain limiting forms of the above equations are of interest.

Case (a). In this case $k_1 \gg (k_d + k_3)$. Under these conditions $p = q = k_1$, $\lambda_2 = 0$, $\lambda_1 = k_1$, and eq A11–A13 reduce to

$$(A)/(A)_0 = e^{-k_1\Delta t} \quad \text{(A14)}$$

$$(B)/(A)_0 = [1 - e^{-k_1\Delta t}] \quad \text{(A15)}$$

$$(C)/(A)_0 \approx 0 \quad \text{(A16)}$$

Equations A14–A16 are, of course, equivalent to eq A7–A8.

Case (b). In this case $(k_1 + k_d) \gg k_3$. Under these conditions $(p - q) = (k_1 + k_d)$, $\lambda_2 = 0$, and $\lambda_1 = (k_1 + k_d)$.

$$\frac{(A)}{(A)_0} = \frac{1}{k_1 + k_d}[k_d + k_1 e^{-(k_1+k_d)\Delta t}] \quad \text{(A17)}$$

$$\frac{(B)}{(A)_0} = \frac{k_1}{k_1 + k_d}[1 - e^{-(k_1+k_d)\Delta t}] \quad \text{(A18)}$$

$$\frac{(C)}{(A)_0} \approx 0 \quad \text{(A19)}$$

If $(k_1 + k_d)\Delta t \gg 1$, then eq A17 and A18 become

$$\frac{(A)}{(A)_0} = \frac{k_d}{k_1 + k_d} \quad \text{(A20)}$$

$$\frac{(B)}{(A)_0} = \frac{k_1}{k_1 + k_d} \quad \text{(A21)}$$

Case (c). In this case $k_1 \ll (k_d + k_3)$. Under these conditions the expression for q may be expanded to give

$$q = p - \frac{2k_1k_3}{p} \quad \text{(A22)}$$

$$\lambda_2 = \frac{k_1k_3}{k_d + k_3} \quad \text{(A23)}$$

Moreover, since $\lambda_1 \gg \lambda_2$, we have

$$\frac{(A)}{(A)_0} = e^{-k_1k_3\Delta t/(k_d+k_3)} \quad \text{(A24)}$$

$$\frac{(B)}{(A)_0} = \frac{k_1}{k_d + k_3}\frac{(A)}{(A)_0} \quad \text{(A25)}$$

$$\frac{(C)}{(A)_0} = 1 - e^{-k_1k_3\Delta t/(k_d+k_3)} \quad \text{(A26)}$$

The above expressions are equivalent to the steady-state approximation for the concentration of B. If the exponents can be expanded, we obtain

$$(A)/(A)_0 = 1 - k_1k_3\Delta t/(k_d + k_3) \quad \text{(A27)}$$

$$(C)/(A)_0 = k_1k_3\Delta t/(k_d + k_3) \quad \text{(A28)}$$

References and Notes

(1) Participant, Brookhaven National Laboratory Summer Student Program, 1978.
(2) For references to the properties of the RuL_3^{2+} excited states see the following recent review articles: (a) Sutin, N.; Creutz, C. *Adv. Chem. Ser.* **1978**, *168*, 1. (b) Sutin, N. *J. Photochem.* **1979**, *10*, 19.
(3) Lin, C-T.; Sutin, N. *J. Phys. Chem.* **1976**, *80*, 97.
(4) Finkenberg, E.; Fisher, P.; Huang, S-M. Y.; Gafney, H. D. *J. Phys. Chem.* **1978**, *82*, 526.
(5) Crosby, G. A.; Klassen, D. M.; Sabath, S. L. *Mol. Cryst.* **1966**, *1*, 453.
(6) Demas, J. N.; Crosby, G. A. *J. Am. Chem. Soc.* **1971**, *93*, 2841.
(7) Demas, J. N.; Harris, E. W.; McBride, R. P. *J. Am. Chem. Soc.* **1977**, *99*, 3547.
(8) Fink, D. W.; Ohnesorge, W. E. *J. Am. Chem. Soc.* **1969**, *91*, 4995.
(9) Kirk, A. D.; Hoggard, P. E.; Porter, G. B.; Rockley, M. G.; Windsor, M. W. *Chem. Phys. Lett.* **1976**, *37*, 199.
(10) Street, A. J.; Goodall, D. M.; Greenhow, R. C. *Chem. Phys. Lett.* **1978**, *56*, 326.
(11) Chum, H. L.; Koran, D.; Osteryoung, R. A. *J. Am. Chem. Soc.* **1978**, *100*, 310.
(12) Phillips, J.; Koningstein, J. A.; Langford, C. H.; Sasseville, R. *J. Phys. Chem.* **1978**, *82*, 622.
(13) Dwyer, F. P.; Gibson, N. A.; Gyarfas, E. C. *J. Proc. R. Soc. N. S. W.* **1952**, *84*, 80.
(14) Ford-Smith, M. H.; Sutin, N. *J. Am. Chem. Soc.* **1961**, *83*, 1830.
(15) Lin, C-T.; Böttcher, W.; Chou, M.; Creutz, C.; Sutin, N. *J. Am. Chem. Soc.* **1976**, *98*, 6536.
(16) Creutz, C. *Inorg. Chem.* **1978**, *17*, 1046.
(17) Netzel, T. L.; Struve, W. S.; Rentzepis, P. M. *Annu. Rev. Phys. Chem.* **1973**, *24*, 473.
(18) Shapiro, S. L., Ed. "Ultrashort Light Pulses"; Springer-Verlag: Heidelberg, 1977.
(19) Alfano, R. R.; Shapiro, S. L. *Phys. Rev. Lett.* **1970**, *74*, 584.
(20) Busch, G. E.; Jones, R. P.; Rentzepis, P. M. *Chem. Phys. Lett.* **1973**, *18*, 178.
(21) Netzel, T. L.; Rentzepis, P. M. *Chem. Phys. Lett.* **1974**, *29*, 337.
(22) Siebert, M. In "Current Topics in Bioenergetics", Vol. 7; Academic Press: New York, 1978.
(23) Magde, D.; Windsor, M. W. *Chem. Phys. Lett.* **1974**, *27*, 31.
(24) Bensasson, R.; Salet, C.; Balzani, V. *J. Am. Chem. Soc.* **1976**, *98*, 3722.
(25) Lachish, U.; Infelta, P. P.; Grätzel, M. *Chem. Phys. Lett.* **1979**, *62*, 317.
(26) Note, however, that both the spectrum and the difference spectrum for $Ru(bpy)_3^{2+}$ below 350 nm differ from the results published in ref 2a.
(27) Palmer, R. A.; Piper, T. S. *Inorg. Chem.* **1966**, *5*, 864.
(28) Brunschwig, B. S.; Sutin, N. *J. Am. Chem. Soc.* **1978**, *100*, 7568.
(29) Maestri, M.; Bolletta, F.; Moggi, L.; Balzani, V. *J. Chem. Soc. Chem. Commun.* **1977**, 491.
(30) Mahon, C.; Reynolds, W. L. *Inorg. Chem.* **1967**, *6*, 1927.
(31) Lever, A. B. P. "Inorganic Electronic Spectroscopy"; American Elsevier: New York, 1968; pp 302–303.
(32) Madeja, K.; König, E. *J. Inorg. Nucl. Chem.* **1963**, *25*, 377.
(33) Although high-spin $Fe(phen)_2X_2$ complexes do undergo metal-to-ligand charge transfer at around 500 nm, these transitions are weak ($\epsilon \ll 10^3\ M^{-1}\ cm^{-1}$).[32]
(34) Chan, M-S.; Wahl, A. C. *J. Phys. Chem.* **1978**, *82*, 2542.
(35) Young, R. C.; Keene, F. R.; Meyer, T. J. *J. Am. Chem. Soc.* **1977**, *99*, 2468.
(36) Saji, T.; Aoyagui, S. *J. Electroanal. Chem.* **1975**, *63*, 31.
(37) Marcus, R. A. *Discuss. Faraday Soc.* **1960**, *29*, 21. *Can. J. Chem.* **1959**,

37, 155. J. Phys. Chem. 1963, 67, 853.
(38) Dexter, D. L. J. Chem. Phys. 1973, 21, 836.
(39) Dose, E. V.; Hoselton, M. A.; Sutin, N.; Tweedle, M. F.; Wilson, L. J. J. Am. Chem. Soc. 1978, 100, 1141.
(40) The Stokes shifts of the emission from the MLCT states of $Ru(bpy)_3^{2+}$ and $Os(bpy)_3^{2+}$ are relatively small: see ref 28.
(41) Konig, E.; Watson, K. J. Chem. Phys. Lett. 1970, 6, 457.
(42) A value of ~0.5 eV is calculated assuming that the Franck-Condon or distortion energy of the excited state is equal to $6f(\Delta a_0)^2/2$ where Δa_0 is the difference between the iron-nitrogen bond lengths in the ground and excited states (0.14 Å) and f is a breathing force constant. The value of f was taken as that of $Fe(H_2O)_6^{2+}$ (1.6×10^5 dyn cm^{-1}; see: Sutin, N. In "Tunneling in Biological Systems", Chance, B., DeVault, D. C., Frauenfelder, H., Marcus, R. A., Schrieffer, J. R., Sutin, N., Eds.; Academic Press: New York, 1979; p 201.
(43) Dwyer, F. P.; Gyarfas, E. C. J. Am. Chem. Soc. 1954, 76, 6320.
(44) The difference between iron-nitrogen distances in $Fe(phen)_3^{2+}$ and $Fe(phen)_3^{3+}$ is less than 0.01 Å (ref 45 and 46).
(45) Zalkin, A.; Templeton, D. H.; Ueki, T. Inorg. Chem. 1973, 12, 1641.
(46) Baker, J.; Engelardt, L. M.; Figgis, B. N.; White, A. H. J. Chem. Soc., Dalton Trans. 1975, 530.
(47) Calculated using 385 cm^{-1} for the iron-nitrogen stretching frequency of $Fe(bpy)_3^{3+}$. See: Saito, Y.; Takemoto, J.; Hutchinson, B.; Nakamoto, K. Inorg. Chem. 1972, 11, 2003.
(48) Observed rates are generally 10^3 times slower than calculated rates in systems of this type (see ref 15 and 28).
(49) Ohsawa, Y.; Saji, T.; Aoyagui, S. J. Electroanal. Chem., submitted for publication.

Influence of Crystal Packing on the $\eta^1 \rightarrow \eta^3$ Rearrangement of an Allyl Ligand. Solution and Solid-State Structures of the Tetraphenylborate and Hexafluorophosphate Salts of a Platinum Allyl Cation

Carolyn Pratt Brock* and Thomas G. Attig

Contribution from the Department of Chemistry, University of Kentucky, Lexington, Kentucky 40506. *Received May 29, 1979*

Abstract: In acetone or methanol solution the reaction of $\{trans\text{-}PtH(solvent)(PEt_3)_2\}^+$ with *trans*-dimethyl 1-methylenecyclopropane-2,3-dicarboxylate affords a single product which is shown by infrared and NMR spectroscopy to contain the $\{Pt[\eta^1\text{-}CH(COOCH_3)C(COOCH_3)=CHCH_3](PEt_3)_2\}^+$ cation. The crystal structure of its tetraphenylborate salt (space group C_{2v}^9-$Pna2_1$, a = 28.302 (5), b = 12.382 (2), c = 12.741 (2) Å) has been determined by conventional X-ray diffraction methods (2267 observations, 300 variables, final R index on F_o of 0.037) and shows the cation to have the η^1-allyl structure given above. In crystals of the hexafluorophosphate salt, however (space group C_{2h}^5-$P2_1/c$, a = 10.191 (2) Å, b = 13.348 (3) Å, c = 21.351 (5) Å, β = 100.02 (2)°, 8314 observations, 307 variables, R index on F_o of 0.034), the cation has the quite different structure $\{Pt[\eta^3\text{-}CH_3CHC(CO_2CH_3)CHCO_2CH_3](PEt_3)_2\}^+$. This $\eta^1 \rightarrow \eta^3$ allyl rearrangement, which in the solid state is dependent on the identity of a noncoordinating anion, is not observed in solution by either infrared or NMR spectroscopy. The change in the dominant form of the cation of the PF_6^- salt upon crystallization is an example of stabilization by crystal packing of a structure which is not important in other phases, and is strong evidence that the η^1 and η^3 structures are related by a low-energy pathway.

Allyl groups usually bond to Pt(II) as either η^1 (I) or η^3 (II) ligands. The effects of ancillary ligands and solvent on the

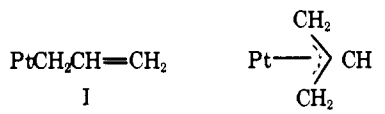

I II

mode of coordination have been described. Trialkylphosphines are more conducive to the formation of η^1 complexes than are triarylphosphines so that under the same reaction conditions oxidative addition of allyl halides to $Pt(PEt_3)_4$ and $Pt(PPh_3)_4$ leads to the isolation of *trans*-$Pt(\eta^1\text{-allyl})X(PEt_3)_2$ and $[Pt(\eta^3\text{-allyl})(PPh_3)_2]^+X^-$, respectively.[1,2] In the specific case of C_3H_5Cl and PPh_3 the neutral η^1 complex appears to be favored in benzene solution while the ionic η^3 form is dominant in chloroform.[3]

NMR studies also suggest that these two modes of coordination are similar energetically. Some η^3-allyl complexes of Pt(II) have been shown to undergo syn-anti exchange which can be slowed at low temperature, and a mechanism involving an η^1-allyl specie as an intermediate has been proposed.[2,4] The structure of a single crystal of *trans*-$Pt(\eta^1\text{-}C_3H_5)Cl(PPh_3)_2$ isolated from a bulk solution of the corresponding dynamic η^3 complex is evidence for such a process.[3] Kurosawa et al.[5] suggest that three intermediates are important in the exchange; a *cis*-η^1-allyl complex, a *trans*-η^1-allyl complex, and a neutral η^3-allyl complex formed by the dissociation of a phosphine followed by the coordination of the halide.

In studies of the cyclopropane ring-opening reaction of Feist's esters by Pt(II) hydrides[6,7] we have found that the product of the reaction is influenced not only by the coordi-

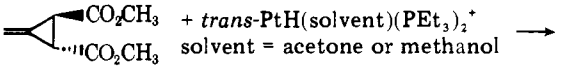

nating ability of the anion and, in solution, by the solvent, but is also influenced in the solid state by packing interactions. Herein we describe the solution and solid-state infrared spectra, NMR spectra, and crystal structures of two cationic Pt(II) allyl complexes which differ only in anion (BPh_4^- and PF_6^-). Although both salts have the η^1 structure in solution, the PF_6^- salt crystallizes as the η^3-allyl; the cation of the BPh_4^- salt is the expected η^1-allyl. To our knowledge this is the first crystallographic study of a system in which the bonding mode of a ligand depends on the identity of a noncoordinating counterion.

Counterion effects in the solid state have been observed previously for both cationic and anionic linkage isomers of SCN^- and $SeCN^-$.[8,9] For example, in the sterically hindered complex $Pd(Et_4dien)X^+$ (Et_4dien = 1,1,7,7-tetraethyldiethylenetriamine; X = SCN^-) the bonding mode of X is anion dependent. In the solid state the BPh_4^- salt is more stable as the S-bonded thiocyanate while the PF_6^- and SCN^- salts are

0002-7863/80/1502-1319$01.00/0 © 1980 American Chemical Society